Participation of Chromatin-Remodeling Proteins in the Repair of Ultraviolet-B-Damaged DNA[1][C][W][OA]

Mabel Campi, Lucio D'Andrea, Julia Emiliani, and Paula Casati*

Centro de Estudios Fotosintéticos y Bioquímicos, Universidad Nacional de Rosario, 2000 Rosario, Argentina

The genome of plants is organized into chromatin, affecting the rates of transcription, DNA recombination, and repair. In this work, we have investigated the consequences of reduced expression of some chromatin-remodeling factors and histone acetylation in maize (*Zea mays*) and Arabidopsis (*Arabidopsis thaliana*) in their participation in DNA repair after ultraviolet (UV)-B irradiation. Plants deficient in *NFC102/NFC4* or *SDG102/SDG26* showed more damaged DNA than wild-type plants; however, the Arabidopsis *chc1* mutant showed similar accumulation of cyclobutane pyrimidine dimers as wild-type plants, in contrast to the increased DNA damage measured in the maize *chc101* RNA interference line. In Arabidopsis, plants deficient in chromatin remodeling are also affected in the accumulation of pigments by UV-B. Plants treated with an inhibitor of histone acetyltransferases, curcumin, previous to the UV-B treatment show deficiencies in DNA repair; in addition, the chromatin remodeling-deficient plants have altered levels of acetylated histones after the UV-B treatment, demonstrating that histone acetylation is important during DNA repair in these two plant species. Arabidopsis mutants *ham1* and *ham2* also showed increased DNA damage after UV-B, suggesting that the role of these proteins in DNA damage repair has been conserved through evolution. However, cyclobutane pyrimidine dimer accumulation was higher in *ham1* than in *ham2*; suggesting that HAM1 has a major role in DNA repair after UV-B. In summary, in this work, we have demonstrated that chromatin remodeling, and histone acetylation in particular, is important during DNA repair by UV-B, demonstrating that both genetic and epigenetic effects control DNA repair in plants.

Genetic information encoded by eukaryotic DNA is compacted into chromatin, allowing the genome to fit within the nucleus (for review, see Pfluger and Wagner, 2007). The basic unit of chromatin is the nucleosome, which is formed by wrapping 147 bp of DNA around a histone octamer. The nucleosomal structure is a barrier to proteins involved in transcription, replication, and DNA recombination and repair; and chromatin must be restructured in order to allow these processes to occur. This is accomplished by three distinct processes that collectively regulate these activities: first, covalent modification of histones, primarily in the N-terminal tails, which is accomplished by suites of histone-modifying enzymes that change histone-DNA interaction and thus change protein-binding affinities; second, chromatin-remodeling complexes that alter histone-DNA interaction, facilitating nucleosome sliding to a new position and inducing conformational changes in histone-DNA interactions as well as histone loss or nucleosome disassembly; and last, methylation of DNA cytosine residues, which obstructs the binding of some proteins and recruits others, including transcription factors (Eberharter and Becker, 2002; Pfluger and Wagner, 2007; Vaillant and Paszkowski, 2007).

The disruption of the nucleosome-DNA interactions or the remodeling of chromatin can stimulate or repress DNA repair. In yeast, RAD54, RAD26, and RDH54, which all belong to the Switch2/Suc Nonfermenting2 (Swi2/Snf2) superfamily, participate in meiosis and also in various aspects of DNA repair, for example in recombination between homologous chromosomes and in nucleotide excision and transcription-coupled repair (Eisen et al., 1995; Klein, 1997; Shinohara et al., 1997). Mutants of RAD54 and of its orthologs in chicken, mouse, and *Schizosaccharomyces pombe* are sensitive to ionizing radiation and to methylmethane sulfonate and are defective in homologous integration of exogenous DNA. Besides, in *Drosophila*, a RAD54 homolog is involved in x-ray resistance and in recombination repair (Bezzubova et al., 1997; Essers et al., 1997; Muris et al., 1997; Kooistra et al., 1997; Arbel et al., 1999). On the other hand, in yeast, rapid DNA repair was measured in various nucleosomal regions of the genome when photolyase was overexpressed, including inactive and active genes and repressed promoters. While heterochromatin was repaired within minutes, centromeres were not repaired; thus, the rapid repair measured in heterochromatin regions suggests that the spontaneous unwrapping of nucleosomes provides

[1] This work was supported by Fondo para la Investigacion Cientifica y Tecnologica (FONCyT; grant nos. PICT–2006–00957 and PICT–2007–00711 to P.C.).

* Corresponding author; e-mail casati@cefobi-conicet.gov.ar.

The author responsible for distribution of materials integral to the findings presented in this article in accordance with the policy described in the Instructions for Authors (www.plantphysiol.org) is: Paula Casati (casati@cefobi-conicet.gov.ar).

[C] Some figures in this article are displayed in color online but in black and white in the print edition.

[W] The online version of this article contains Web-only data.

[OA] Open Access articles can be viewed online without a subscription.

www.plantphysiol.org/cgi/doi/10.1104/pp.111.191452

DNA access to photolyase activity (Bucceri et al., 2006). In humans, the UV-sensitivity disorder Cockayne syndrome is caused by a defect in CSB, a RAD26 homolog with ATP-dependent chromatin-remodeling activity (Troelstra et al., 1992; Citterio et al., 2000). In Arabidopsis (*Arabidopsis thaliana*), alteration in the expression of *MIM*, a gene encoding a chromatin structural component related to the maintenance of chromosomes, affects the rate of intrachromosomal recombination (Hanin et al., 2000); and BRU1, another chromatin-related gene, participates both in heterochromatin stability to gene silencing and in DNA repair (Takeda et al., 2004). The involvement of the Arabidopsis SWI2/SNF2 gene family in DNA recombination and repair has also been demonstrated (Fritsch et al., 2004). In addition, Shaked et al. (2006) showed that 14 of the 40 Arabidopsis SWI2/SNF2 gene family members also had a role in DNA damage response against γ or UV-C radiation and recombination.

All these results have demonstrated the participation of chromatin remodeling in DNA repair and recombination in different species. However, even if the DNA-repair machinery is usually well conserved during evolution and plants seem to have the same complement of repair enzymes as other species (Britt and May, 2003), there are significant differences between them. For example, homologous recombination is less efficiently used for double-strand break repair in plants than in yeast, while nonhomologous end joining is the prominent pathway used (Gorbunova and Levy, 1999). Moreover, mutations that are lethal in other species are viable in plants, like RAD50 (Gallego and White, 2001), MRE11 (Gallego et al., 2001; Bundock and Hooykaas, 2002), or AtERCC1 (Hefner et al., 2003; Dubest et al., 2004).

Sessile plants are constantly exposed to diverse environmental perturbations, and to survive, they must acclimate to abiotic conditions such as excessive or inadequate light, water, salt, and temperature. Because plants capture light for photosynthesis, they also experience fluctuating solar UV-B radiation (280–315 nm), and this energetic radiation causes direct damage to DNA, proteins, lipids, and RNA (Britt, 1996; Gerhardt et al., 1999; Casati and Walbot, 2004). Absorption of UV-B by DNA induces the formation of covalent bonds between adjacent pyrimidines, giving rise to cyclobutane pyrimidine dimers (CPD) and, to a lesser extent, pyrimidine pyrimidone photoproducts (Friedberg et al., 1995). These lesions have been shown to disrupt base pairing and block DNA replication and transcription if photoproducts persist, or they result in mutations if photoproducts are bypassed by error-prone DNA polymerases (Britt, 1996). Thus, the accumulation of such lesions must be prevented to maintain genome integrity, plant growth, and seed viability. Moreover, plants lack a reserved germ line, and mutations occurring in somatic cells could be transmitted to the progeny. Therefore, plants have not only evolved mechanisms that filter or absorb UV-B to protect them against DNA damage (Mazza et al., 2000; Bieza and Lois, 2001) but also have different DNA-repair systems to remove or tolerate DNA lesions (Hays, 2002; Bray and West, 2005; Kimura and Sakaguchi, 2006).

In maize (*Zea mays*), chromatin remodeling has been implicated in UV-B responses, a discovery from transcriptome profiling of lines differing in UV-B sensitivity. Because there is less air mass and greater atmospheric transparency to shorter wavelengths, plants at high altitudes generally experience higher UV-B radiation flux (Madronich et al., 1995). We previously reported that maize landraces from high altitudes have adaptations (specific alleles) that increase UV-B tolerance; for example, they constitutively express higher levels of genes predicted to encode chromatin-remodeling factors than temperate zone lines and then acclimate by showing greater UV-B-mediated upregulation of these genes (Casati et al., 2006). To test the hypothesis that chromatin-remodeling capacity is important, transgenic plants (in the temperate B73 inbred) expressing RNA interference (RNAi) to reduce four chromatin-remodeling factors were found to be acutely sensitive to UV-B at doses that do not cause visible damage to maize lacking flavonoid sunscreens. These lines were knockdown for *chc101*, *nfc102*, *sdg102*, and *mbd101* genes. *chc101* encodes a putative component of the SWI/SNF and Remodel the Structure of Chromatin (RSC) chromatin-remodeling complex; CHC101 is a SWIB domain-containing protein and is a likely homolog of yeast Swp73 and Rsc6 proteins and human SMARD proteins. *mbd101* encodes a putative methyl-CpG-binding domain (MBD) protein. *nfc102* encodes a member of the nucleosome/chromatin-assembly factor group C, which is a RBP4/7 homolog; it is highly similar to the human retinoblastoma-binding protein RbBp48, a WD-40 protein found in several chromatin regulatory complexes. And *sdg102* encodes a SET domain protein; it is a putative histone H3 Lys-36 histone methyltransferase from the ASH1 group. Even though the precise roles of CHC101, NFC102, SDG102, and MBD101 have not been demonstrated in maize, the compelling biology is that all knockdown plants are hypersensitive to UV-B: symptoms included necrotic sun burning of adult tissue, decreased photosynthetic pigments, altered expression of some UV-B-regulated genes, and seedling lethality (Casati et al., 2006). These RNAi-expressing lines showed no symptoms under visible light, while nontransgenic siblings in a UV-B-tolerant temperate zone line (B73) lacked symptoms under UV-B (Casati et al., 2006). At the chromatin level, mass spectrometry analysis of post-translational histone modifications demonstrated that UV-B-tolerant B73 and high-altitude landraces exhibit greater acetylation of N-terminal H3 and H4 tails after irradiation than UV-B-sensitive temperate (W23 background) and RNAi knockdown lines (Casati et al., 2008). In addition, microarray analysis was done using two of these RNAi maize lines in the absence and presence of UV-B; these lines exhibit substantially different transcriptome changes, despite both exhibiting identical

phenotypic consequences after UV-B exposure (Casati and Walbot, 2008). Therefore, chromatin-remodeling capacity is important for effective responses to UV-B, and the loss of capacity is associated with hypersensitivity.

In this work, the consequences of the reduced expression of four maize chromatin genes, *chc101*, *nfc102*, *sdg102*, and *mbd101*, were analyzed in relation to their participation in DNA repair after UV-B irradiation in maize. In addition, Arabidopsis mutants and RNAi lines in the ortholog genes were also compared with regard to their role in DNA repair. Finally, because histone H3 and H4 acetylation is increased by UV-B (Casati et al., 2008), the effect of histone acetylation on DNA repair was also analyzed in both plant species; in particular, the role of a group of Arabidopsis histone acetyltransferases, HAM1 and HAM2, in DNA damage repair was investigated.

RESULTS

Chromatin Remodeling-Deficient Maize Plants Show Increased UV-B Induced DNA Damage

As described in the introduction, we have previously shown that transgenic maize plants expressing RNAi to reduce the expression of four chromatin factors, *chc101*, *nfc102*, *sdg102*, and *mbd101*, were acutely sensitive to UV-B at doses that do not cause visible damage to maize lacking flavonoid sunscreens (Casati et al., 2006). However, microarray analysis using two of these RNAi maize lines, *chc101* and *mbd101*, after 8 h of UV-B and under control conditions in the absence of UV-B, showed that these plants exhibit substantially different transcriptome changes despite both exhibiting identical phenotypic consequences after UV-B exposure (Casati and Walbot, 2008). Chromatin-remodeling activities have been previously proposed to participate in DNA repair in different organisms, including plants (Hanin et al., 2000; Takeda et al., 2004; Shaked et al., 2006). Nevertheless, none of these activities have been demonstrated to participate in the repair of UV-B-induced DNA damage. Thus, the participation of maize CHC101, NFC102, SDG102, and MDB101 in the repair of CPDs was assayed in plants that were treated with UV-B radiation for 8 h. Wild-type plants in the B73 background and the maize knockdowns in the four chromatin-remodeling genes were grown in the greenhouse in the absence of UV-B for 4 weeks, and they were then treated with UV-B radiation for 8 h (2 W m^{-2}). As a control, different sets of plants were irradiated with the same lamps covered with a polyester plastic that absorbs UV-B (see "Materials and Methods"). Leaf samples from control and treated plants were collected immediately after, or 4 and 24 h after, the end of the treatment under light conditions that allow photoreactivation. DNA was extracted and CPD abundance was compared in each line after the UV-B treatment, and also relative to CPD levels in B73 plants, by an immunologically sensitive assay; this assay detects CPDs by monoclonal antibodies specifically raised against them. DNA at 1.5 μg was used for each sample, as there is a linear relationship of signal values of UV-B-treated samples versus the corresponding amounts of DNA loaded up to 2 μg of DNA (Lario et al., 2011). Comparison of CPD accumulation in samples from B73 and the knockdown plants after the 8-h UV-B treatment, and 4 h after the end of the UV-B treatment, relative to levels under control conditions in the absence of UV-B are shown in Figure 1A. In the absence of UV-B, the steady-state levels of CPDs in B73 and chromatin remodeling-deficient plants were similar (optical density of about 200 in all samples). After 8 h of exposure with UV-B, unrepaired lesions accumulated in all plants (Fig. 1A); however,

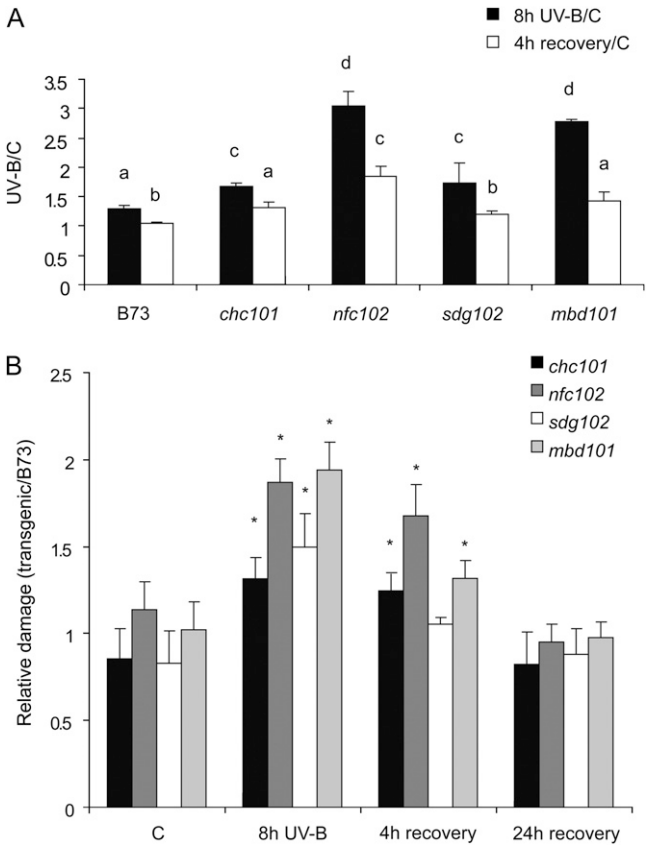

Figure 1. CPD levels in the DNA of wild-type (B73) and knockdown maize plants in chromatin-remodeling genes. A, CPD levels in DNA of UV-B-treated B73, *chc101*, *nfc102*, *sdg102*, and *mbd101* knockdown RNAi plants for 8 h and after a recovery period in the absence of UV-B for 4 h, relative to the levels under control conditions without UV-B (C). B, CPD levels in DNA of *chc101*, *nfc102*, *sdg102*, and *mbd101* knockdown RNAi plants relative to B73 plants under control conditions without UV-B (C), after an 8-h UV-B treatment or after a recovery period in the absence of UV-B for 4 or 24 h. Experiments were done under conditions that allowed photorepair in the light. A total of 1.5 μg of DNA was loaded in each well. Results represent averages ± SD of six independent biological replicates. Different letters denote statistical differences applying an ANOVA test using Sigma Stat 3.1 ($P < 0.05$). Asterisks denote statistical differences applying Student's *t* test ($P < 0.05$).

the accumulation of CPDs in the knockdown plants was more severe than in B73. Although photoreactivation is evident in all lines after 4 h of recovery, most of the transgenic plants still show more CPDs than B73 plants at this time (Fig. 1A). Figure 1B shows CPD accumulation in each knockdown plant under control conditions in the absence of UV-B and after the different UV-B treatments compared with levels in B73 plants. Immediately after an 8-h UV-B treatment, the chromatin remodeling-deficient lines accumulated 44% (*chc101*), 87% (*nfc102*), 50% (*sdg102*), and 94% (*mbd101*) more CPDs than B73 plants (Fig. 1B). After 4 h of recovery in the absence of UV-B, CPD levels in most of the transgenic lines were still higher than in B73 plants; only *sdg102* showed similar CPD levels as B73 (Fig. 1B), demonstrating that the repair of UV-B-induced DNA lesions is less efficient in the absence of these chromatin-remodeling factors. However, after 24 h of recovery, CPD levels in all the chromatin remodeling-deficient lines were similar to those in the B73 line, indicating that after 1 d in the absence of UV-B, knockdown plants can recover similarly to wild-type plants.

UV-B Regulation of Arabidopsis Chromatin-Remodeling Proteins, Mutant Analysis, and Physiological Effects

To further investigate the role of this subset of chromatin-remodeling proteins in UV-B damage responses in plants, we looked for the Arabidopsis orthologs of *chc101*, *nfc102*, *sdg102*, and *mbd101* to test if these chromatin activities in DNA repair are conserved between plant species. For this, we performed a BLAST analysis using the Plant Chromatin database (http://www.chromdb.org/) for mRNA and protein Arabidopsis sequences showing the highest homologies with the maize sequences. For maize *CHC101*, the highest identity at the nucleotide level was found with Arabidopsis *CHC1* (At5g14170; 55% identity for the corresponding open reading frames [ORFs]), showing a 66% identity at the amino acid level (Supplemental Fig. S1, A and B). For *NFC102*, the BLAST analysis resulted in the identification of an Arabidopsis homolog, *NFC4*, also known as *MSI4/FVE* (At2g19520; Hennig et al., 2005), showing a 74% identity for the corresponding ORF and 77% identity at the protein level (Supplemental Fig. S1, C and D); and for maize *SDG102*, we found that Arabidopsis *SDG26* or *ASHH1* (At1g76710) showed the highest homology, with 43% identity for the corresponding ORF and 55% identity at the protein level (Supplemental Fig. S1, E and F). When the reciprocal BLAST analysis was done (identification of maize genes with the highest homology with Arabidopsis genes), the same transcripts/proteins were identified (http://www.chromdb.org/). When a BLAST analysis was done for *MBD101*, we were not able to identify any Arabidopsis ORF sequence with any significant homology. However, at the protein level, we found that MDB101 is 37% identical to Arabidopsis MBD4, but when ORF alignments were done between *MDB101* and *MBD4* (At3g63030), only a short sequence of 32 bases showed 84% identity, with a total identity of 5% (Supplemental Fig. S1, G and H). Because of the low homology at both cDNA and protein levels of *MBD101*/MBD101 and *MBD4*/MBD4, this chromatin-remodeling activity in Arabidopsis was not further analyzed.

All four maize chromatin-remodeling genes, *chc101*, *nfc102*, *sdg102*, and *mbd101*, were reported to be induced by UV-B (Casati et al., 2006); thus, we investigated if the Arabidopsis orthologs were similarly regulated. Wild-type plants of the Columbia-0 ecotype grown in the absence of UV-B were exposed under UV-B lamps for 4 h (2 W m^{-2}) in a growth chamber. After the treatment, leaf tissue from 4-week-old plants was collected for RNA extraction and quantitative reverse transcription (qRT)-PCR analysis. Like their maize orthologs, *CHC1*, *NFC4*, and *SDG26* were up-regulated by UV-B (Fig. 2). To further investigate the role of these three proteins in the repair of UV-B-induced DNA lesions, several Arabidopsis mutants defective in *CHC1*, *NFC4*, and *SDG26* genes were identified in the SALK, SAIL, and RNAi knockdown from the Functional Genomics of Chromatin: Global Control of Plant Gene Expression collections (http://www.chromdb.org/rnai/rnai_lines_info.html). For *CHC1*, two independent T-DNA insertional lines, SAIL_1186_A10 (*chc1-1*) and SALK_113834 (*chc1-2*), with insertions in the 5′ untranslated region and the first intron, respectively, were identified (Supplemental Fig. S2) by a PCR screen using gene-specific primers and one specific primer for the T-DNA left border (Table I). Insertional inactivation of *CHC1* in the *chc1-1* line was confirmed by RT-PCR (Supplemental Fig. S2). The consequences of insertion of the T-DNA in the first intron of the *CHC1* gene in *chc1-2* were confirmed by qRT-PCR on homozygous plants for the mutant allele (Supplemental Fig. S2). The results indicate that the *CHC1* transcript abundance in the *chc1-2* mutant line was two times lower than in wild-type plants. For the *NFC4* gene, an RNAi line was obtained from the Plant Chromatin collection (*nfc4-1*); RNAi plants had four times lower levels of *NFC4* transcripts than wild-type plants (Supplemental Fig. S3). A T-DNA insertion mutant in the 11th exon was also obtained (SAIL_1167_E05; *nfc4-2*). Supplemental Figure S2 shows that homozygous plants had undetectable levels of *NFC4* transcripts when analyzed by RT-PCR. For the *SDG26* gene, a T-DNA insertion in the fifth exon was obtained (SALK_013895; *sdg26-1*). Supplemental Figure S2 shows that homozygous plants had undetectable levels of *SDG26* transcripts when analyzed by RT-PCR. A second RNAi transgenic line was obtained from the Plant Chromatin collection (*sdg26-2*); these plants had 2.6-fold decreased *SDG26* levels in comparison with wild-type plants (Supplemental Fig. S3).

Because RNAi maize transgenic plants with lower expression of such chromatin-associated genes exhibited hypersensitivity to UV-B by increased leaf chlorosis and necrosis (Casati et al., 2006), we investigated the effects of a UV-B treatment on physiological parameters in the

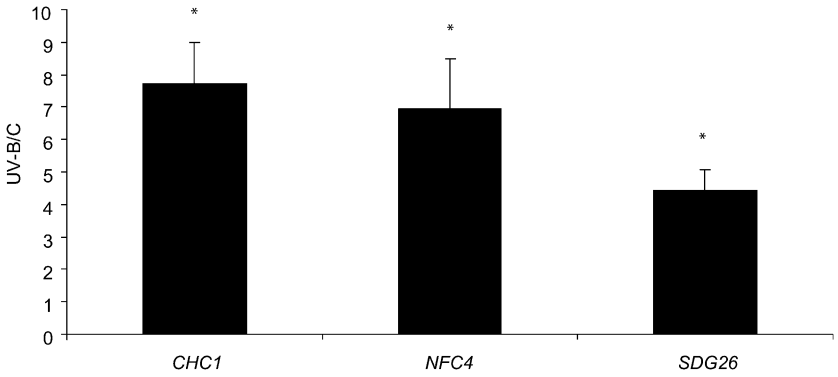

Figure 2. Relative transcript levels of Arabidopsis chromatin-remodeling genes measured by qRT-PCR. Plants were irradiated with UV-B light for 4 h (UV-B) or kept under control conditions (C) as indicated in "Materials and Methods." Data show means ± SD of at least three independent experiments. Asterisks denote statistical differences applying Student's *t* test ($P < 0.05$).

Arabidopsis mutants. UV-B induces flavonoids and other UV sunscreens in many plants (Li et al., 1993; Landry et al., 1995; Ormrod et al., 1995). After UV-B irradiation, the concentration of these molecules is 54% higher than under control conditions in wild-type plants (Fig. 3A). On the contrary, the chromatin remodeling-deficient mutants showed minor (24% for *chc1-1*) or no increase (*nfc4-1* and *sdg26-1*) in UV sunscreen levels after the treatment (Fig. 3A). However, when pigment levels were compared in baseline control conditions in the absence of UV-B, *sdg26* mutants showed already elevated flavonoid levels similar to those in wild-type plants after the UV-B treatment. Thus, plants with decreased levels of the chromatin-remodeling factors under study have altered regulation of UV sunscreen accumulation. Also, when chlorophyll pigments were measured after the UV-B treatment, there was no overall significant effect on wild-type plants or the *nfc4* and *sdg26* mutants (Fig. 3B); on the contrary, *chc1* mutants showed decreased amounts of both chlorophyll *a* and *b*, with no changes in the chlorophyll *a*/*b* ratio, suggesting that at the doses used in our experiments, UV-B induces leaf chlorosis in these plants. In addition, UV-B sensitivity was analyzed by the inhibition of primary root elongation (Tong et al., 2008). After only 1 d of UV-B treatment, wild-type seedlings showed a significant decrease in primary root elongation (Fig. 3C). However, *chc1* plants showed a slight but still significant lower decrease in primary root growth than wild-type plants, which was observed 2 d after the end of the UV-B treatment, in sharp contrast to *sdg26* seedlings, which showed a similar inhibition of primary root elongation by UV-B to wild-type plants (Fig. 3E). On the contrary, under control conditions in the absence of UV-B, the *nfc4* mutants showed a significant decrease in primary root elongation compared with wild-type plants; however, after the UV-B treatment, the root elongation rate was similar in both plants (Fig. 3D), suggesting that these mutants are less responsive to UV-B radiation than wild-type plants.

Chromatin-Remodeling Proteins in UV-B Damage DNA Repair in Arabidopsis

To test if the participation of the chromatin activities under study in UV-B-induced DNA repair is conserved between plant species like maize and Arabidopsis, we grew Arabidopsis wild-type plants and the mutants in a growth chamber in the absence of UV-B for 4 weeks, and plants were then exposed to UV-B for 4 h (2 W m^{-2}). As a control, different sets of plants were irradiated with the same lamps covered with a polyester plastic that absorbs UV-B. Leaf samples from control and treated plants were collected immediately after, and 4 or 24 h after, the end of the UV-B treatment. DNA was extracted and the CPD abundance was assayed after the different treatments. As measured in maize plants, UV-B induced a CPD accumulation in all lines, including wild-type plants (Fig. 4A). Comparison of CPD accumulation in samples from wild-type and mutant plants after the UV-B treatment and under control conditions in the absence of UV-B showed that, in the absence of UV-B, the steady-state levels of CPDs in the wild type and all mutants were similar (Fig. 4B). However, after 4 h of UV-B exposure, more CPDs accumulated in *nfc4* and *sdg26* lines than in the wild-type plants (Fig. 4B; Supplemental Fig. S4A). On the contrary, *chc1* mutants did not show any significant change in the accumulation of UV-B-damaged DNA in comparison with wild-type plants (Fig. 4B; Supplemental Fig. S4A). Thus, NFC4 and SDG26 prob-

Table I. *Primers used for the identification of homozygous mutant lines*

Name	Sequence
LB-SALK	5′-GTCCGCAATGTGTTATTAAGTTGTC-3′
LB-SAIL	5′-TTCATAACCAATCTCGATACAC-3′
LP_*chc1*	5′-AAAATACGGGTCGGGTCT-3′
RP_*chc1*	5′-GTGGCCATAGAAAGATCTGG-3′
LP_*nfc4-1*	5′-TGTCCGGTTGTTTGATCGTA-3′
RP_*nfc4-1*	5′-CACGATCAGACTTCTTACTG-3′
LP_*sdg26-1*	5′-TGATTTCGGAGACCCTGA-3′
RP_*sdg26-1*	5′-TTGAGCCCTCTTCTTTGC-3′
LP_*ham1-1*	5′-TTATTGGGCCACACTCCTT-3′
RP_*ham1-1*	5′-TTGAATTGCAAAGCCCTCT-3′
LP_*ham1-2*	5′-CTGTTTCCCATTCACGACA-3′
RP_*ham1-2*	5′-TCACCGGATGGTATTTTCC-3′
LP_*ham2-1*	5′-GGAAGACAAGGTGCGTTCT-3′
RP_*ham2-1*	5′-ATGCCTTTGAAGCTGCTCT-3′
LP_*ham2-2*	5′-TTTTCTTTCTTTTTGCCACA-3′
RP_*ham2-2*	5′-GCTGACGATCCCATTTCTC-3′

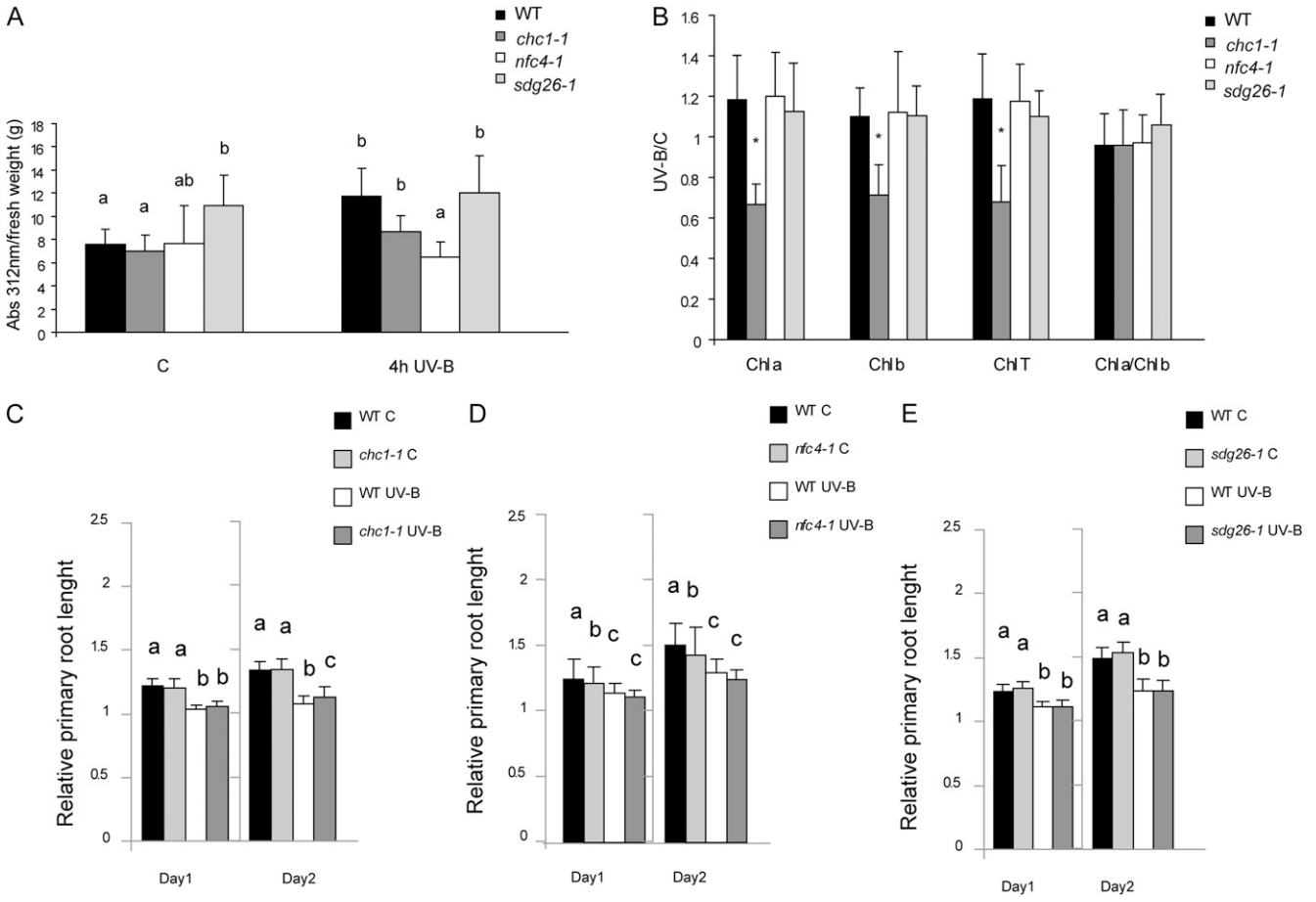

Figure 3. A and B, Total UV-B-absorbing compounds (A), as well as chlorophyll *a* and *b*, total chlorophyll, and chlorophyll *a*/*b* ratio (B), were assayed after 4 h of UV-B (UV-B) compared with untreated controls (C) in wild-type plants (WT) and *chc1*, *nfc4*, and *sdg26* mutants. Measurements are averages of six adult leaves from six different plants. C to E, Phenotypic analysis of the wild type and *chc1* (C), *nfc4* (D), and *sdg26* (E) mutants. Seedlings were grown vertically for 7 d on Murashige and Skoog plates. Graphs show average primary root lengths in wild-type, *chc1*, *nfc26*, and *sdg26* plants, relative to the root length measured immediately after the UV-B treatment ($n = 20$ for all genotypes). Error bars represent SD. Statistical significance was analyzed using ANOVA and Tukey's tests with $P < 0.05$; differences from the control are marked with letters or asterisks.

ably have a similar role in the repair of UV-B-damaged DNA as their maize orthologs, but not CHC1, or at least not under the conditions of our experiments. Maize and Arabidopsis plants deficient in NFC102 and NFC4 activities, respectively, are the most sensitive UV-B lines (Figs. 1B and 4B); while plants deficient in SDG102 and SDG26 activities show less CPD accumulation by UV-B than NFC102- and NFC4-deficient plants, but statistically significantly higher levels of CPDs than wild-type plants. After 4 and 24 h of recovery in the absence of UV-B, CPD levels in the Arabidopsis mutants were similar to those in wild-type plants (Fig. 4B), indicating that after 4 h in the absence of UV-B, the mutants can recover similarly to wild-type plants.

To discard the possibility that the mutations in *SDG26* and *NFC4* genes may be affecting the expression of DNA-repair enzymes of other repair systems, *UVR2* (encoding a CPD photolyase; At1g12370) and *UVR7* (encoding ERCC1, a DNA excision repair protein of the nucleotide excision repair system; At3g05210) transcript levels were analyzed by qRT-PCR in all the lines under study. Similar levels of both transcripts were measured in wild-type and mutant plants, both under control conditions and after the 4-h UV-B treatment (Supplemental Fig. S5). These results indicate that major CPD removal mechanisms are unaffected in mutant plants.

Collectively, these results suggest that chromatin-remodeling activities participate in CPD removal in both maize and Arabidopsis; however, differences in the participation of chromatin-remodeling activities in DNA repair exist between both species.

Role of Histone Acetylation in Chromatin Remodeling

Next, we investigated the role of histone acetylation in the repair of CPDs provoked by UV-B. Previously, by mass spectrometry analysis of histone proteins, we demonstrated that acetylation of histone H3 and H4 N-terminal tails is increased in UV-B-treated maize

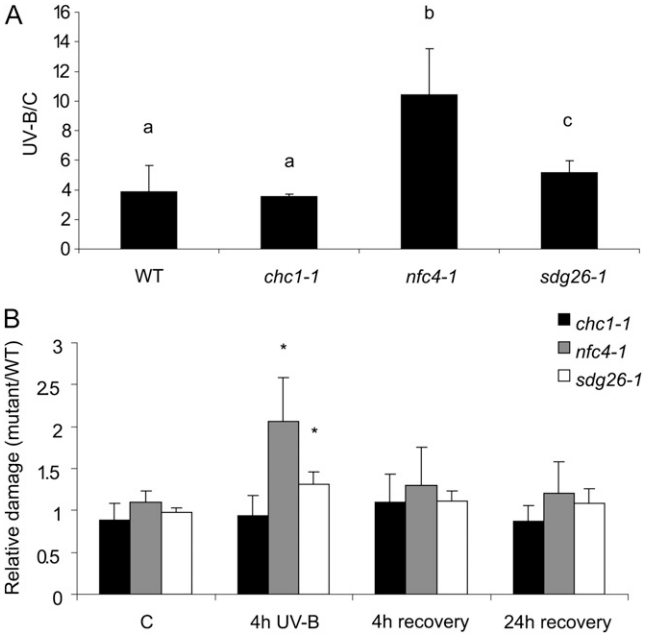

Figure 4. CPD levels in the DNA of wild-type and mutant Arabidopsis plants in chromatin-remodeling genes. A, CPD levels in DNA of UV-B-treated wild-type (WT), *chc1*, *nfc4*, and *sdg26* mutant plants for 4 h relative to levels under control conditions without UV-B (C). B, CPD levels in DNA of *chc1*, *nfc4*, and *sdg26* mutant plants relative to wild-type plants under control conditions without UV-B (C) after a 4-h UV-B treatment or after a recovery period in the absence of UV-B for 4 or 24 h. Experiments were done under conditions that allowed photorepair in the light. A total of 1.5 μg of DNA was loaded in each well. Results represent averages ± SD of six independent biological replicates. Different letters denote statistical differences applying an ANOVA test ($P < 0.05$). Asterisks denote statistical differences applying Student's *t* test ($P < 0.05$).

plants (Casati et al., 2008). Similar results were also described in yeast, where UV irradiation triggers genome-wide histone hyperacetylation at both histone H3 and H4, while histone hyperacetylation diminishes gradually as repair proceeds (Yu et al., 2005). To confirm that histone acetylation is important during DNA repair of CPDs in plants, we treated the maize B73 line with 100 μM curcumin, an inhibitor of histone acetylation (Balasubramanyam et al., 2004; Casati et al., 2008), immediately prior to the UV-B treatment. DNA was extracted then, immediately after the UV-B treatment, and 4 h after the end of the treatment for CPD quantification. Figure 5A shows that if histone acetylation is impaired, there is an increased accumulation of CPDs by UV-B; this accumulation is still measured 4 h after the end of the UV-B treatment. Thus, blocking a specific aspect of chromatin remodeling, histone acetylation prior to the UV-B treatment, dampens the mechanisms of DNA repair. A similar experiment was done using wild-type plants and *chc1* and *sdg26* Arabidopsis mutants to test if different activities in chromatin remodeling act synergistically with histone acetylation during DNA repair. As measured in maize, after 4 h of UV-B, plants treated with curcumin showed increased accumulation of CPDs compared with levels in untreated plants (Fig. 5B); this is true for both wild-type and mutant plants. However, the *sdg26* mutants, which accumulate higher levels of CPD by UV-B than wild-type plants (Figs. 4B and 5B), showed more CPDs than wild-type plants when pretreated with curcumin, suggesting that both histone acetylation and histone methylation act synergistically during DNA repair by UV-B. On the contrary, *chc1* mutants did not show significant differences from wild-type plants when pretreated with curcumin (Fig. 5B). Together, these experiments indicate that failure to achieve histone acetylation impairs the repair of DNA damage.

sdg102/26, *nfc102/4*, *chc101*, and *mbd101* Plants Are Deficient in Histone Acetylation

Because we have here demonstrated that histone acetylation is required for UV-B-induced DNA damage repair in maize and Arabidopsis, we then analyzed histone acetylation levels in our chromatin remodeling-deficient plants. By western-blot analysis using antibodies against acetylated histone H3 in the N-terminal domain, it is clear that maize plants from the B73 genotype show increased acetylation of this histone after an 8-h UV-B treatment, as we reported previously by mass spectroscopy analysis (Casati et al., 2008). However, *chc101*, *nfc102*, *sdg102*, and *mbd101* plants showed lower levels of H3 acetylation after the UV-B treatment than wild-type plants (Fig. 6, A and B). When this experiment was repeated using Arabidopsis plants, similar results were obtained: wild-type plants showed an increase in histone acetylation after the UV-B treatment, while the mutants, with the exception of *chc1* plants, showed a lower or no increase in the levels of acetylated H3 (Fig. 6, C and D).

To demonstrate that the decrease in histone acetylation in the mutants after the UV-B treatment can be at least one cause of the decreased efficiency in DNA repair of these mutants, chromatin immunoprecipitation (ChIP) analysis using antibodies against acetylated H3 and H4 in the N-terminal domains followed by dot-blot experiments using antibodies against CPDs were done, to quantify the CPD accumulation in the DNA associated with equal levels of acetylated histones. Figure 7 shows that, despite higher levels of CPDs being accumulated in the RNAi plants when total and input DNA are measured, or when DNA is immunoprecipitated using antibodies that recognize total pools of histone H4, when DNA associated with acetylated histones is immunoprecipitated, CPD levels in equal amounts of the immunoprecipitated DNA are similar in all lines. Together, our experiments demonstrate that the mutants do not show an increase in histone acetylation after the UV-B treatment (or show a minor increase compared with wild-type plants). Because when histones are acetylated DNA is repaired more efficiently, these lower acetylation levels measured

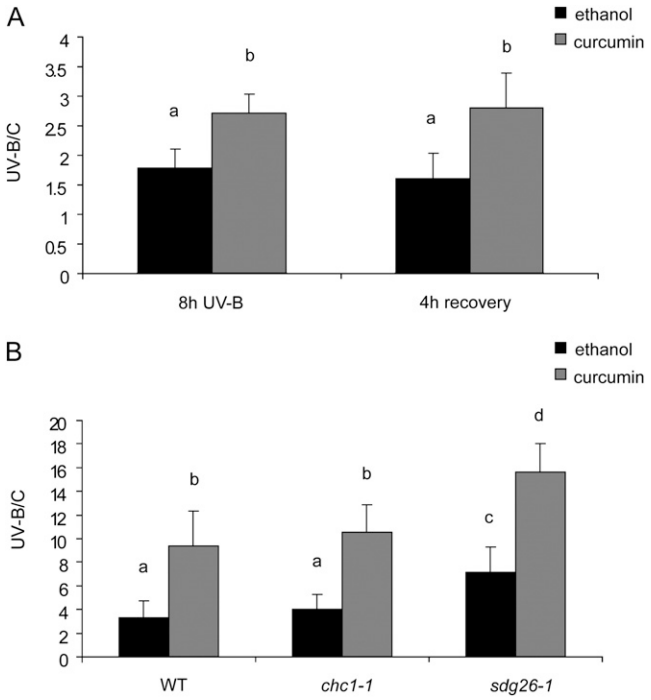

Figure 5. CPD levels in the DNA of maize and Arabidopsis plants pretreated with curcumin, a histone acetylase inhibitor. A, CPD levels in DNA of UV-B-treated B73 maize plants for 8 h or after a 4-h recovery relative to levels under control conditions without UV-B (C). Plants were pretreated with curcumin or ethanol as a control. B, CPD levels in DNA of UV-B-treated wild-type, *chc1*, and *sdg26* mutant Arabidopsis plants for 4 h relative to levels under control conditions without UV-B (C). Plants were pretreated with curcumin or ethanol as a control. Experiments were done under conditions that allowed photorepair in the light. A total of 1.5 μg of DNA was loaded in each well. Results represent averages ± SD of six independent biological replicates. Different letters denote statistical differences applying an ANOVA test ($P < 0.05$).

in the mutants may be at least one cause of their deficiency to repair UV-B-damaged DNA.

DNA Repair in Arabidopsis Requires the Activity of HAM1 and HAM2 Histone Acetyltransferases

We finally investigated the role of two Arabidopsis histone acetyltransferases of the MYST family, HAM1 (At5g64610) and HAM2 (At5g09740), in DNA repair. In Arabidopsis, there are at least 10 different histone acetyltransferases that are grouped in three families: the CBP family (HAC; five members), the GNAT superfamily (HAG; three members), and the MYST family (HAM; two members [http://www.chromdb.org]). Each of these enzymes can acetylate different residues in either or both H3 and H4, giving them specificity. In humans, the best-characterized member of the MYST family is TIP60 (from Tat-interacting protein of 60 kD). TIP60 has important roles during DNA repair, transactivating genes in response of DNA damage, and more importantly, acetylating H4 when DNA is damaged (Squatrito et al., 2006). The Arabidopsis genome encodes two closely related MYST family proteins, HAM1 and HAM2 (87.9% identity and 92.5% similarity in amino acid sequences; Supplemental Fig. S6); both proteins show around 40% identity with human TIP60 (Supplemental Fig. S6). Also, HAM1 and HAM2 are functionally redundant, as single Arabidopsis *ham1* and *ham2* mutants display a wild-type phenotype, while no double mutant seedling can be recovered (Latrasse et al., 2008). In our experiments, after 4 h of UV-B, both genes are induced in wild-type plants (Fig. 8A). Thus, we looked for Arabidopsis plants that were deficient in the expression of these genes in the SALK and RNAi knockdown stock from the Plant Chromatin consortium (http://www.chromdb.org/rnai/rnai_lines_info.html). For *HAM1*, two independent T-DNA insertional lines, SALK_027726 (*ham1-1*) and SALK_147727 (*ham1-2*), with insertions in the first exon and the promoter, respectively, were identified (Supplemental Fig. S2). Insertional inactivation of *HAM1* in the *ham1-1* line was confirmed by RT-PCR (Supplemental Fig. S2). The consequences of insertion of the T-DNA in the

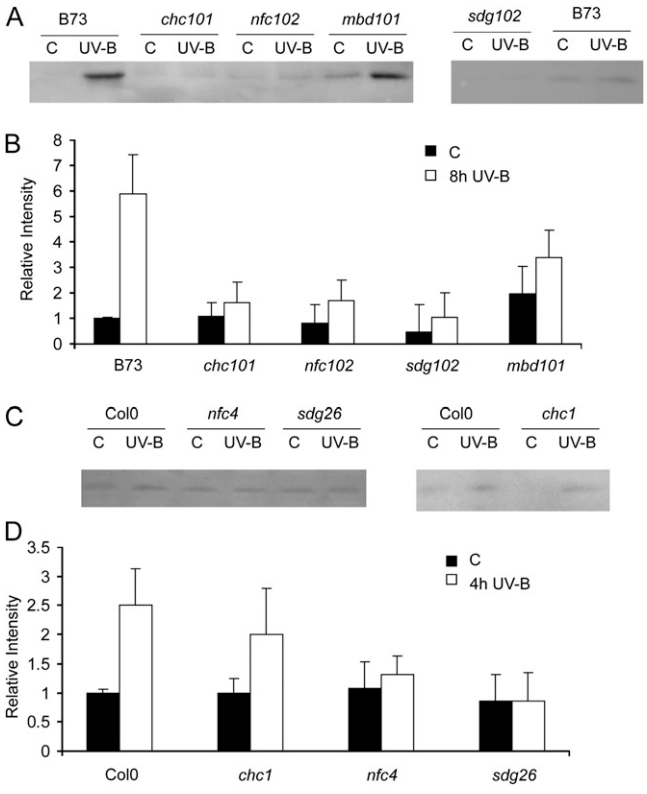

Figure 6. Western-blot analysis of histone extracts from maize and Arabidopsis plants. A and C, Total histones were extracted as described by Casati et al. (2008) and used in western-blot analysis using antibodies against acetylated H3 in the N-terminal domain. B and D, Densitometric analyses of the western blots. Results represent averages ± SD of at least three independent biological replicates. C indicates control data in all panels.

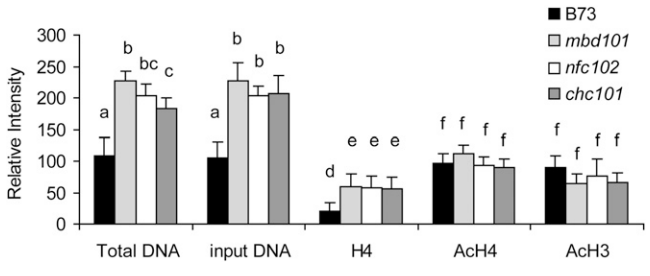

Figure 7. CPD levels in the DNA of wild-type B73, *chc101*, *nfc102*, and *mbd101* maize plants. CPD levels are shown in total DNA, input DNA, and coimmunoprecipitated DNA using antibodies against H4, acetylated H4 (AcH4), and acetylated H3 (AcH3) of UV-B-treated plants. Experiments were done under conditions that allowed photorepair in the light. A total of 4 ng of coimmunoprecipitated DNA was loaded in each well. Results represent averages ± SD of at least three independent biological replicates. Different letters denote statistical differences applying an ANOVA test ($P < 0.05$).

promoter of the *ham1-2* line was confirmed by qRT-PCR on plants homozygous for the mutant allele (Supplemental Fig. S2), showing that the *HAM1* transcript abundance in *ham1-2* was 2-fold lower than in wild-type plants. For the *HAM2* gene, a T-DNA insertion in the second intron was obtained from the Delarue laboratory (Latrasse et al., 2008; SALK_106046; *ham2-1*). Supplemental Figure S2 shows that homozygous plants had undetectable levels of *HAM2* transcripts when analyzed by RT-PCR. A second mutant line (SALK_012086) was also obtained, with a T-DNA insertion in the promoter region (*ham2-2*). This line has similar *HAM2* transcript levels to wild-type plants under control growth conditions in the absence of UV-B (Supplemental Fig. S2); however, when mutant plants were UV-B irradiated, plants showed 20 times lower *HAM2* mRNA levels than wild-type plants under the same conditions. Thus, the T-DNA insertion in the promoter region of the *ham2-2* mutant affects its regulation by UV-B radiation, so we also included this line in our analysis. Finally, an RNAi knockdown from the Plant Chromatin consortium was also obtained, which shows decreased expression of both *HAM1* and *HAM2* (2- and 1.6-fold, respectively; *ham1/ham2*; Supplemental Fig. S3). Mutant plants in *HAM1* showed decreased levels of UV-B-absorbing pigments under control conditions in the absence of UV-B (Fig. 8B). After a 4-h UV-B treatment, while wild-type plants showed an increase in UV-B-absorbing pigments, both mutants showed significantly lower levels than wild-type plants (Fig. 8B). However, the RNAi knockdown did not show differences in UV-B-absorbing compound levels compared with the wild type (Fig. 8B). While *ham2* mutants did not show any significant decrease in chlorophyll levels after the UV-B treatment, *ham1* mutants showed lower levels of these pigments after the treatment (Fig. 8C).

To test if histone acetylation by HAM1 and HAM2 proteins is important during UV-B-induced DNA repair, Arabidopsis wild-type plants and the *ham1* and *ham2* plants were exposed to 4 h of UV-B radiation. As a control, plants were irradiated with the same lamps covered with a polyester plastic that absorbs UV-B. Leaf samples from control and treated plants were collected immediately after, and 24 h after, the end of the UV-B treatment; DNA was extracted and the CPD abundance was measured. UV-B induced a CPD accumulation in all lines (Fig. 9A). Comparison of the CPD levels in samples from wild-type and mutant plants in control conditions in the absence of UV-B showed that the steady-state levels of CPDs in all plants were similar (Fig. 9B). After 4 h of UV-B, more CPDs accumulated in the *ham1* and *ham2* lines than in the wild-type plants (Fig. 9B; Supplemental Fig. S4B). However, CPD levels were higher in the *ham1* mutant than in the *ham2* mutant or the RNAi plants (Fig. 9B).

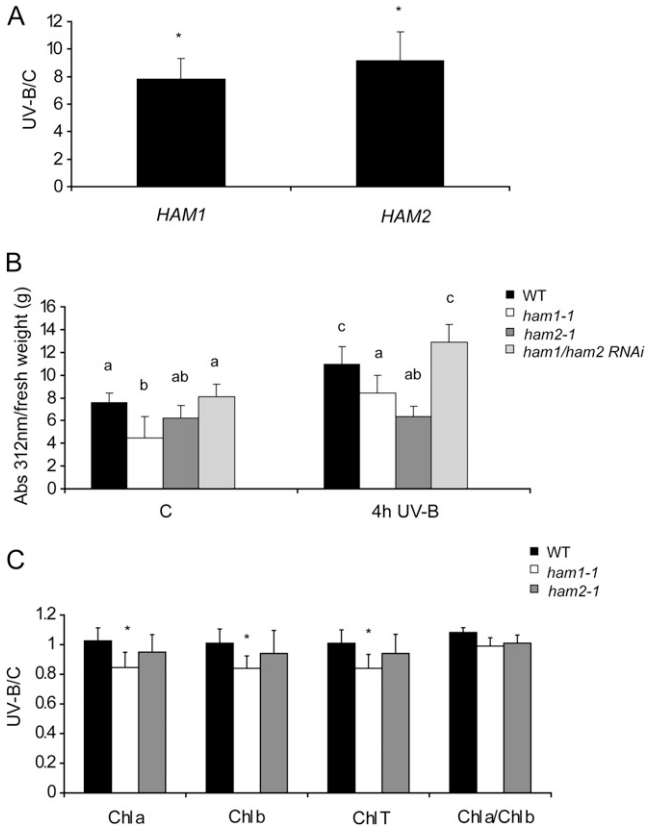

Figure 8. A, Relative transcript levels of *HAM1* and *HAM2* measured by qRT-PCR. Wild-type plants were irradiated with UV-B light for 4 h (UV-B) or kept under control conditions (C) as indicated in "Materials and Methods." Data show means ± SD of at least three independent experiments. Asterisks denote statistical differences applying Student's *t* test ($P < 0.05$). B and C, Total UV-B-absorbing compounds (B), as well as chlorophyll *a* and *b*, total chlorophyll, and chlorophyll *a*/*b* ratio (C), were assayed after 4 h of UV-B compared with untreated controls (C) in wild-type plants (WT) and *ham1* and *ham2* mutants. Measurements are averages of six adult leaves from six different plants ± SD. Statistical significance was analyzed using a paired *t* test or an ANOVA test with $P < 0.05$; differences from the control are marked with asterisks or different letters.

UVR2 and *UVR7* levels were also analyzed in *ham1* and *ham2* mutants. As for the other mutants analyzed in this work, similar levels of both transcripts were measured in wild-type and mutant plants, both under control conditions and after the 4-h UV-B treatment (Supplemental Fig. S5), indicating that major CPD removal mechanisms are unaffected in mutant plants.

Interestingly, after 24 h of recovery in the absence of UV-B, CPD levels in the *ham1* mutants were still higher than in wild-type plants, while *ham2* mutants showed a similar recovery as detected in wild-type plants, with RNAi plants still showing some damage compared with the wild type but less than *ham1* mutants (Fig. 9B); this demonstrates that HAM1 has a major role in DNA repair after UV-B, as occurs with TIP60 in humans (Squatrito et al., 2006).

DISCUSSION

Absorption of UV-B radiation by DNA induces the formation of covalent bonds between adjacent pyrimidines, giving rise to cyclobutane pyrimidine dimers and, to a lesser extent, pyrimidine pyrimidone photoproducts (Friedberg et al., 1995); overaccumulation of these lesions must be prevented to maintain genome integrity, plant growth, and seed viability. Moreover, plants lack a reserved germ line, and mutations occurring in somatic cells could be transmitted to the progeny. Therefore, plants have not only evolved mechanisms that filter or absorb UV-B to protect them against DNA damage (Mazza et al., 2000; Bieza and Lois, 2001) but also have DNA-repair systems to remove DNA lesions (Hays, 2002; Bray and West, 2005; Kimura and Sakaguchi, 2006). The genome of plants is organized into chromatin, a structure that limits the accessibility of DNA, affecting the rates of processes such as DNA recombination and repair. Thus, disrupting the nucleosome-DNA interactions or remodeling of chromatin may stimulate DNA repair.

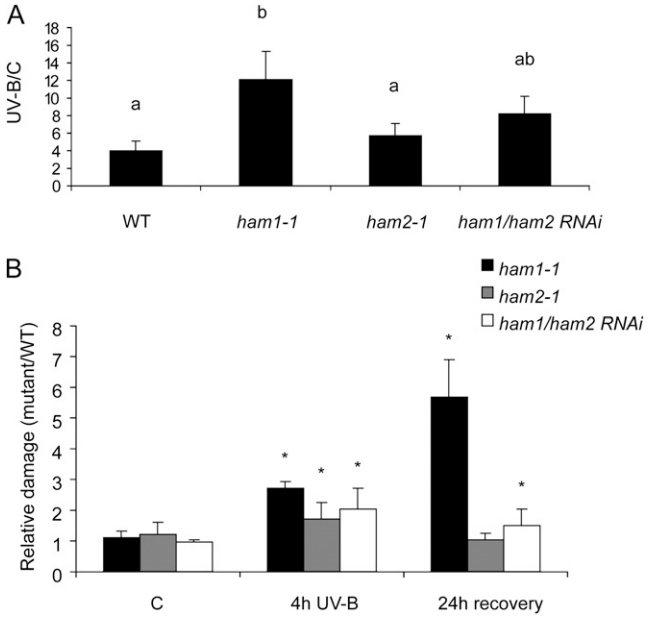

Figure 9. CPD levels in the DNA of wild-type and *HAM1*- and *HAM2*-deficient Arabidopsis plants. A, CPD levels in DNA of UV-B-treated wild-type (WT), *ham1-1*, and *ham2-1* plants and *ham1/ham2* RNAi plants for 4 h (UV-B) relative to levels under control conditions without UV-B (C). B, CPD levels in DNA in *ham1-1*, *ham2-1*, and *ham1/ham2* RNAi plants relative to wild-type plants under control conditions without UV-B (C), after a 4-h UV-B treatment, or after a recovery period in the absence of UV-B for 24 h. Experiments were done under conditions that allowed photorepair in the light. A total of 1.5 μg of DNA was loaded in each well. Results represent averages ± SD of six independent biological replicates. Different letters denote statistical differences applying an ANOVA test ($P < 0.05$). Asterisks denote statistical differences applying Student's *t* test ($P < 0.05$).

In this paper, we have demonstrated that maize and Arabidopsis plants showing reduced or null expression of some chromatin-remodeling factors show increased levels of DNA damage after UV-B irradiation. These plants do not show increased histone acetylation (or show only a lower increase compared with wild-type plants) after the UV-B treatment (Fig. 10). In addition, plants treated with an inhibitor of histone acetyltransferases, curcumin, previous to the UV-B treatment show deficiencies in DNA repair, demonstrating that histone acetylation is important during DNA repair in these two plant species (Fig. 10). Thus, both genetic and epigenetic effects control DNA repair in plants.

In maize, chromatin remodeling has been implicated in UV-B responses. Transgenic maize plants knocked down for chromatin-remodeling genes were found to be acutely sensitive to UV-B at doses that do not cause visible damage to maize lacking flavonoid sunscreens (Casati et al., 2006). However, microarray analysis using two chromatin remodeling-deficient maize lines (*chc101* and *mbd101*) after UV-B irradiation demonstrated that these lines exhibit substantially different transcriptome changes, despite both exhibiting identical phenotypic consequences after UV-B exposure (Casati and Walbot, 2008). Thus, in this work, we have investigated the consequences of the reduced expression of some chromatin-remodeling factors and histone acetylation in maize and Arabidopsis, and their roles in UV-B responses were analyzed in relation to their participation in DNA repair. In maize, all knockdown plants showed increased DNA damage compared with wild-type plants after a UV-B treatment. Arabidopsis plants showed higher UV-B sensitivity than maize plants (Lario et al., 2011); thus, a shorter treatment was used for this species. Still, CPD accumulation after this shorter treatment was higher in wild-type Arabidopsis than in wild-type maize plants (Figs. 1 and 4). Plants deficient in the expression of *NFC102/NFC4* and *SDG102/SDG26* showed increased levels of CPDs compared with wild-type plants; however, the Arabidopsis *chc1* mutant showed similar CPD accumulation to wild-type plants, in contrast to the increased DNA damage

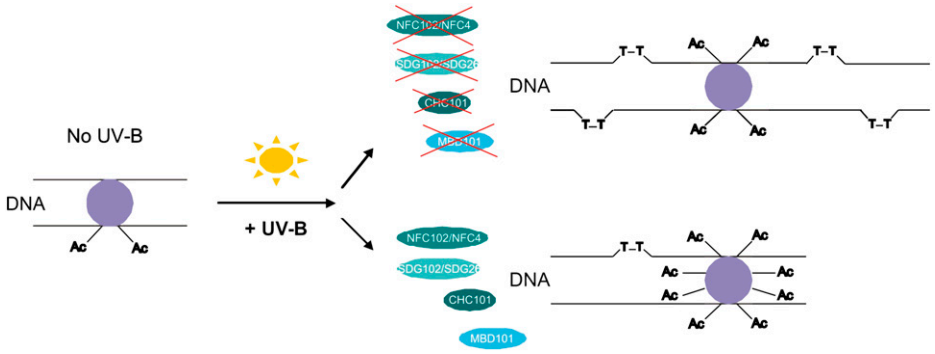

Figure 10. A model depicting epigenetic changes in the chromatin of maize and Arabidopsis wild-type and chromatin-deficient plants after UV-B. Purple circles represent nucleosomes. [See online article for color version of this figure.]

measured in the maize knockdown *chc101* RNAi line (Figs. 1 and 4). Thus, the activities of SDG102/SDG26 and NFC102/NFC4 in DNA repair are probably more important than that of CHC101/CHC1, and the UV-B-related phenotypes associated with a deficiency in the expression of *CHC101/CHC1* are probably not related to their participation in DNA repair. After 24 h of recovery in the absence of UV-B, all maize and Arabidopsis mutants show similar levels of CPD to those in wild-type plants, demonstrating that they can all recover properly.

Arabidopsis NFC4 is also known as FVE. FVE is one of five Arabidopsis MSI1-like genes, which are homologous to the eukaryotic MSI1 family of the WD40 domain-containing proteins found in several protein complexes acting on chromatin (Hennig et al., 2005). *FVE* encodes a homolog of the mammalian retinoblastoma-associated protein, a component of a histone deacetylase complex involved in transcriptional repression (Brehm et al., 1998; Nicolas et al., 2000). FVE participates in a protein complex, repressing *FLC* transcription through a histone deacetylation mechanism (Ausín et al., 2004; Pazhouhandeh et al., 2011). Mutants in this gene show increased levels of *FLC* mRNA, resulting in a photoperiod-independent flowering delay; *fve* mutants flower later than wild-type plants in any photoperiod condition. This increase in *FLC* transcript levels parallels a local decrease in H3K27me3 and an increase in histone H3 acetylation (Pazhouhandeh et al., 2011). In our study, we found that *nfc4* mutants show lower levels of histone acetylation after a UV-B treatment than wild-type plants (Fig. 6). Thus, the measured decrease in global H3 acetylation by UV-B in our studies may seem contrary to the reported increased local H3 acetylation in *FLC* in the mutants. However, it is possible that local changes in acetylated H3 do not reflect global levels of this histone form in the genome. In addition, in the *nfc4* mutants after a UV-B treatment, a different histone deacetylase may be induced to compensate the absence of FVE, and its activity may be responsible for the decreased histone acetylation levels measured in these plants. On the other hand, FVE is a sensor of cold stress in plants (Kim et al., 2004); dual roles of FVE in regulating flowering time and the stress response to cold may provide evolutionary fitness to plants, particularly in enduring the cold spell of early spring. Recently, FVE (or NFC4) has also been implicated in chromatin silencing (Bäurle and Dean, 2008).

Arabidopsis SDG26 is a histone methyltransferase that, in vitro, can methylate oligonucleosomes (Xu et al., 2008). This protein is localized in the nucleus, and loss-of-function *sdg26* mutants show a late-flowering phenotype. These mutants show up-regulation of several MADS-box flowering repressors, including *FLC*; thus, like NFC4, SDG26 acts as a regulator of flowering time control (Xu et al., 2008). Although a function of CHC1 has not been reported, Arabidopsis lines harboring RNAi constructs targeted against *CHC1* were analyzed for their ability to support genetic transformation of roots by *Agrobacterium tumefaciens*. Two independent lines targeting the chromodomain of protein CHC1 showed a severely dwarfed phenotype when grown either in soil or in culture; these lines also were highly refractory to *Agrobacterium*-mediated transformation in all three standard transformation assays. These data suggest that transformation requires DNA synthesis and mitosis in growing tissues and that CHC1 is necessary for these processes (Crane and Gelvin, 2007). Despite all the different roles described for the chromatin proteins investigated in this work, none of them have previously been reported to have a function in DNA repair.

In plants, the first line of defense when exposed to UV-B is the synthesis of protective pigments. In our experiments, flavonoid levels increased in wild-type Arabidopsis plants after the UV-B treatment, while

Table II. *Primers used for RT-qPCR*

Name	Sequence
LP_At_*CHC1*	5′-TCCTCAGGAAGGCTTTGA-3′
RP_At_*CHC1*	5′-CAATCCCGAGAACATCCA-3′
LP_At_*NFC4*	5′-TGGGCACCAAGATAATGC-3′
RP_At_*NFC4*	5′-GGTTTGTGCCAGTTCTCG-3′
LP_At_*SDG26*	5′-TCGCTCAGAAGCATGTTG-3′
RP_At_*SDG26*	5′-TTCTCCGCCACACTTGTT-3′
LP_At_*HAM1*	5′-CGGAGATGCGAATCAGAA-3′
RP_At_*HAM1*	5′-TTCCGTTTCTGGTGTCGT-3′
LP_At_*HAM2*	5′-TGAAGAGCTGGATCCAGCA-3′
RP_At_*HAM2*	5′-CTTTGATATGAAGGCAGGGTT-3′
LP_At_*CPK3*	5′-CGCTGAGAACCTTTCTGAAG-3′
RP_At_*CPK3*	5′-CCATCTCCATCCATATCAGC-3′

chc1 plants showed a smaller increment, and *nfc4* and *sdg26* mutants did not show significant changes. This demonstrates that Arabidopsis plants deficient in chromatin remodeling are affected in the accumulation of UV-absorbing compounds, as described previously in maize chromatin remodeling-deficient plants (Casati et al., 2006). On the other hand, the chlorophyll content of UV-B-treated plants was not affected in the wild type or *nfc4* and *sdg26* mutants, but plants lacking CHC1 showed significantly lower levels of total chlorophyll after the treatment, similar to maize *CHC101*-deficient plants (Casati et al., 2006). Together, and as we described previously in chromatin remodeling-deficient maize plants, Arabidopsis mutants have altered accumulation of pigments by UV-B.

Because histone H3 and H4 acetylation is increased by UV-B (Casati et al., 2008), the effect of histone acetylation on DNA repair was also analyzed. Our results demonstrate that when plants are pretreated with curcumin, a histone acetylase inhibitor, DNA repair is impaired (Fig. 5). Thus, histone acetylation is important during DNA repair in these two plant species. In *sgd26* mutants, curcumin treatment previous to UV-B irradiation induced a significantly higher accumulation of CPDs than curcumin-treated wild-type plants. A deficiency in the expression of the product of the *SDG26* gene, which encodes a histone methyltransferase, interferes either directly or indirectly with the DNA damage repair mediated by histone acetylation. This suggests that both processes, histone acetylation and methylation, act synergistically during UV-B-induced damage repair. In our experiments, we found that all chromatin-deficient plants showing increased UV-B-damaged DNA show decreased levels of acetylated histones after the UV-B treatment compared with wild-type plants. Because when histones are acetylated DNA is repaired more efficiently, the decrease in the acetylation levels measured in the mutants may be at least one cause of their deficiency to repair UV-B-damaged DNA.

The balance of histone acetylation is maintained by the action of histone acetyltransferases and histone deacetylases. In Arabidopsis, there are at least 10 different acetyltranferases; these have been mostly linked to transcriptional regulation. For example, GCN5 plays a role in the regulation of cold tolerance, floral development, embryonic cell-fate patterning, and light responsiveness (Stockinger et al., 2001; Benhamed et al., 2003, 2006; Vlachonasios et al., 2003; Long et al., 2006), while members of the CBP family are involved in regulating flowering time (Han et al., 2007). Recently, a role of Arabidopsis HAM1 and HAM2, two MYST histone acetyltransferases, in gametophyte development was demonstrated (Latrasse et al., 2008). HAM1 and HAM2 possess an in vitro HAT activity specific for Lys-5 of histone H4 (H4K5; Earley et al., 2007). *HAM1* and *HAM2* are apparently functionally redundant, as single Arabidopsis *ham1* and *ham2* mutants display a wild-type phenotype, while no double mutant seedling could be recovered. *ham1ham2* double mutants show severe defects in the formation of male and female gametophytes, resulting in an arrest of the mitotic cell cycle at early stages of gametogenesis (Latrasse et al., 2008). In humans, TIP60 is the best-characterized member of the MYST family. TIP60 plays a key role in DSB repair and is required to maintain genomic integrity and regulate the repair of DNA damage; inactivation of *TIP60* leads to increased sensitivity to ionizing radiation and induces increased levels of chromosomal aberrations (for review, see Sun et al., 2010). In our experiments, Arabidopsis plants deficient in the expression of *HAM1* and *HAM2* also showed increased DNA damage after a 4-h UV-B treatment, suggesting that the role of this protein in DNA damage repair has been conserved through evolution. However, CPD accumulation was higher in the *ham1* mutant than in the *ham2* mutant; after 24 h of recovery in the absence of UV-B, CPD levels in the *ham1* mutants were still higher than in the wild type, while *ham2* mutants showed a total recovery, suggesting that HAM1 has a major role in DNA repair after UV-B.

In summary, in this work, we have demonstrated that chromatin remodeling, and histone acetylation in particular, is important during DNA repair by UV-B. Complex and multiple facets of chromatin remodeling may participate in this process, demonstrating that both genetic and epigenetic effects control DNA repair in plants.

MATERIALS AND METHODS

Plant Material, Growth Conditions, and Irradiation Protocols

Maize (*Zea mays*) RNAi transgenic lines were obtained from the Maize Genetics Stock Center (http://maizecoop.cropsci.uiuc.edu). The transgenic lines are in a hybrid, mainly B73 background, and each contains an RNAi construct directed toward a specific target gene (http://www.chromdb.org/). For *chc101* plants, stock 3201-01 T-MCG3348.02 was used; for *nfc102*, 3201-07 T-MCG3480.04 was used; for *mbd101*, 3201-11 T-MCG3818.11 was used; and for *sdg102*, 3201-15 T-MCG4268.12, 3201-16 T-MCG4268.16, and 3201-17 T-MCG4268.2 were used. Seeds for each transgenic line were planted and resistance to BASTA herbicide was scored; this trait is encoded on the same plasmid as the RNAi expression cassette and hence is a tightly linked marker. The RNAi lines were propagated by pollinating an RNAi carrier with a nontransgenic sibling, resulting in families segregating 1:1 in the subsequent generation. Transgenic plants were validated with three assays: the BASTA herbicide resistance test, PCR detection of the transgene, and verification of reduced target transcript levels using qRT-PCR. Amalgamations of transgenic or nontransgenic siblings from related families segregating for the same RNAi construct were used in some analyses. The maize plants were grown in a greenhouse with supplemental visible light (1,000 mE m^{-2} s^{-1}) under a 15-h/9-h light/dark regime without UV-B for 28 d. UV-B was provided once for 8 h, starting 3 h after the beginning of the light period, using fixtures mounted 30 cm above the plants (Phillips F40UVB 40 W and TL 20 W/12) at a UV-B intensity of 2 W m^{-2} and a UV-A intensity of 0.65 W m^{-2}. The bulbs were covered with cellulose acetate to exclude wavelengths of less than 280 nm. As a control, plants were exposed for 8 h under the same lamps covered with polyester film (no UV-B treatment; UV-B at 0.04 W m^{-2} and UV-A at 0.4 W m^{-2}). Lamp output was recorded using a UV-B/UV-A radiometer (UV203 A +B radiometer; Macam Photometrics) to ensure that both the bulbs and filters provided the designated UV dosage in all treatments. Adult leaf samples were collected immediately after irradiation or 24 h after the end of the UV-B treatment.

Arabidopsis (*Arabidopsis thaliana*) ecotype Columbia and Wassilewskija lines were used for the experiments. The RNAi transgenic lines and the T-DNA insertion mutants were obtained from the Arabidopsis Biological Resource Center. The T-DNA insertion mutants were obtained from the SALK T-DNA insertion mutant collection (Alonso et al., 2003), while the SAIL T-DNA insertion mutant collection was obtained from The European Arabidopsis Stock Center. Mutant lines used are shown in Supplemental Figure S2. Arabidopsis seeds were sown directly on soil and placed at 4°C in the dark. After 3 d, pots were transferred to a greenhouse and plants were grown at 22°C under a 16-h/8-h light/dark regime. Plants were exposed for 4 h to UV-B radiation from UV-B bulbs (2 W m^{-2} UV-B and 0.65 W m^{-2} UV-A; Bio-Rad) in a growth chamber. The bulbs were covered with cellulose acetate to exclude wavelengths of less than 280 nm. Control plants were treated with the same bulbs covered with a polyester film. Adult leaf samples were collected immediately after irradiation or 4 or 24 h after the end of the UV-B treatment.

For the curcumin experiments, leaves from the different plants were sprayed with a solution of 100 μM curcumin in 100% (v/v) ethanol or with 100% (v/v) ethanol as a control, immediately prior to the UV-B or control treatment.

Identification of Insertional T-DNA Mutants

The genotypes of plants with T-DNA constructs were determined using a PCR-based approach. Initial screening was performed using genomic DNA isolated from adult leaves by a modified cetyl-trimethyl-ammonium bromide method (Sambrook and Russel, 2001) and three combinations of primers. Two primers hybridize to specific genomic sequences (Table I), and one primer is located inside the left border of the T-DNA. The presence or absence of the T-DNA insertion in the genes allowed the identification of homozygous, heterozygous, and wild-type plants.

RT-PCR for expression analyses in the knockout T-DNA lines was carried out in a 25-μL final volume containing 1× Taq DNA polymerase buffer, 3 mM $MgCl_2$, 0.2 mM deoxyribonucleotide triphosphate, 0.25 μM of each primer, and 0.625 unit of Taq DNA polymerase (Invitrogen). Cycling were performed under the following conditions: 2 min of denaturation at 95°C; 35 cycles of 15 s of denaturation at 95°C, 20 s of annealing at 57°C, and 30 s of amplification at 72°C; and a final 7 min of amplification at 72°C. RT-PCR products were separated on a 2% (w/v) agarose gel and stained with SYBR Green (Invitrogen).

qRT-PCR

Total RNA was isolated from about 100 mg of tissue using the TRIzol reagent (Invitrogen) as described by the manufacturer's protocol. The RNA was incubated with RNase-free DNase I (1 unit μL^{-1}) following the protocol provided by the manufacturer to remove possible genomic DNA. Then, RNA was reverse transcribed into first-strand cDNA using SuperScript II reverse transcriptase (Invitrogen) and oligo(dT) as a primer. The resultant cDNA was used as a template for qPCR amplification in a MiniOPTICON2 apparatus (Bio-Rad), using the intercalation dye SYBR Green I (Invitrogen) as a fluorescent reporter and Platinum Taq Polymerase (Invitrogen). Primers for each of the genes under study were designed using PRIMER3 software (Rozen and Skaletsky, 2000) in order to amplify unique 150- to 250-bp products (Table II). Amplification was carried out under the following conditions: 2 min of denaturation at 94°C; 40 to 45 cycles at 94°C for 15 s, 57°C for 20 s, and 72°C for 20 s; followed by 10 min of extension at 72°C. Three replicates were performed for each sample. Melting curves for each PCR were determined by measuring the decrease of fluorescence with increasing temperature (from 65°C to 98°C). PCR products were run on a 2% (w/v) agarose gel to confirm the size of the amplification products and to verify the presence of a unique PCR product. Gene expression was normalized to the Arabidopsis calcium-dependent protein kinase 3 (*CPK3*; Table II). The expression of this gene has been reported previously to remain unchanged by UV-B (Ulm et al., 2004).

DNA Damage Analysis

The induction of CPD was determined using an assay described in detail previously (Stapleton et al., 1993). Monoclonal antibodies specific to CPDs (TDM-2) were from Cosmo Bio. After treatment, plant samples (0.1 g) were collected, immediately immersed in liquid nitrogen, and stored at −80°C. A total of 1.5 μg of the extracted DNA by a modified cetyl-trimethyl-ammonium bromide method was denatured in 0.3 M NaOH for 10 min and 6-fold dot blotted onto a nylon membrane (Perkin-Elmer Life Sciences). The membrane was incubated for 2 h at 80°C and then blocked in Tris-buffered saline (TBS; 20 mM Tris-HCl, pH 7.6, and 137 mM NaCl) containing 5% dried milk for 1 h at room temperature or overnight at 4°C. The blot was then washed with TBS and incubated with TDM-2 (1:2,000 in TBS) overnight at 4°C with agitation. Unbound antibody was washed away, and secondary antibody (Bio-Rad) conjugated to alkaline phosphatase (1:3,000) in TBS was added. The blot was then washed several times, followed by the addition of the detection reagents nitroblue tetrazolium and 5-bromo-4-chloro-3-indolyl phosphate. Quantification was achieved by densitometry of the dot blot using ImageQuant software version 5.2. DNA concentration was fluorometrically determined using the Qubit dsDNA assay kit (Invitrogen) and checked on a 1% (w/v) agarose gel stained with SYBR Safe after quantification.

ChIP Analysis

ChIP analyses were performed as described by Casati et al. (2008).

Immunoblot Analysis

For immunodetection, total histones were extracted as described by Casati et al. (2008). Fifteen percent (w/v) SDS-PAGE was performed, and proteins were electroblotted onto a nitrocellulose membrane for immunoblotting according to Burnette (1981). Commercial IgG fractions were used for the detection of acetylated histone H3 (Upstate). Bound antibody was visualized by linking to alkaline phosphatase-conjugated goat anti-rabbit/anti-mouse IgG according to the manufacturer's instructions (Bio-Rad). The molecular masses of the polypeptides were estimated from a plot of the log of the molecular masses of marker standards (Bio-Rad) versus migration distance.

Root Length Measurements

Surface-sterilized seeds were grown on Murashige and Skoog growth medium on petri dishes. Plates were placed at 4°C in the dark for 3 d, and they were then held vertical in a growth chamber. Seedlings were grown at 22°C under a 16-h/8-h light/dark regime for 7 d and were UV-B treated for 70 min (3 W m^{-2} UV-B and 0.65 W m^{-2} UV-A). Control seedlings were treated under the same lamps covered with polyester film (UV-B at 0.02 W m^{-2} and UV-A at 0.4 W m^{-2}). Plates were kept in the absence of UV-B for 2 d, and they were then photographed daily. Images were analyzed using the ImageJ program. Primary root lengths were determined by measuring the length of a line traced along the root.

Pigment Measurements

UV-absorbing pigments (A_{312}) were determined as described by Casati and Walbot (2004). Total chlorophylls were determined by standard procedures (Wintermans and de Mots, 1965).

Statistical Analysis

Statistical analysis was done using ANOVA models (Tukey's test) using untransformed data or, alternatively, by paired Student's *t* test.

Sequence data from this article can be found in the GenBank/EMBL data libraries under accession numbers NM_121421, NM_127510, NM_106321, NM_125857, NM_121011, NM_001175516, NM_001111597, NM_001112195, and NM_001111702.

Supplemental Data

The following materials are available in the online version of this article.

Supplemental Figure S1. Alignment of the coding and amino acid sequences of maize and Arabidopsis chromatin-remodeling proteins.

Supplemental Figure S2. Locations of the T-DNA insertions and polymorphisms in the *CHC1*, *NFC4*, *SDG26*, *HAM1*, and *HAM2* genes and analysis of their transcript levels.

Supplemental Figure S3. Relative transcript levels of Arabidopsis chromatin-remodeling genes measured by qRT-PCR in wild-type plants and in *nfc4* (A), *sdg26* (B), and *ham1/ham2* (C and D) RNAi transgenic plants.

Supplemental Figure S4. CPD levels in the DNA of *chc1-2*, *nfc4-2*, and *sdg26-2* (A) and *ham1-2* and *ham2-2* (B) mutants relative to wild-type Arabidopsis plants after a 4-h UV-B treatment.

Supplemental Figure S5. Relative expression of *UVR2* and *UVR7* transcripts by qRT-PCR.

Supplemental Figure S6. Amino acid sequence alignment of human TIP60 and Arabidopsis HAM1 and HAM2 (A) and similarity percentages between the human and Arabidopsis proteins (B).

ACKNOWLEDGMENTS

We thank the Arabidopsis Biological Resource Center for providing SALK seed stocks, M. Delarue for providing the SALK_106046 mutant, and the Maize Genetics Stock Center for the RNAi transgenic lines.

Received November 23, 2011; accepted December 14, 2011; published December 14, 2011.

LITERATURE CITED

Alonso JM, Stepanova AN, Leisse TJ, Kim CJ, Chen H, Shinn P, Stevenson DK, Zimmerman J, Barajas P, Cheuk R, et al (2003) Genome-wide insertional mutagenesis of *Arabidopsis thaliana*. Science **301:** 653–657

Arbel A, Zenvirth D, Simchen G (1999) Sister chromatid-based DNA repair is mediated by RAD54, not by DMC1 or TID1. EMBO J **18:** 2648–2658

Ausín I, Alonso-Blanco C, Jarillo JA, Ruiz-García L, Martínez-Zapater JM (2004) Regulation of flowering time by FVE, a retinoblastoma-associated protein. Nat Genet **36:** 162–166

Balasubramanyam K, Varier RA, Altaf M, Swaminathan V, Siddappa NB, Ranga U, Kundu TK (2004) Curcumin, a novel p300/CREB-binding protein-specific inhibitor of acetyltransferase, represses the acetylation of histone/nonhistone proteins and histone acetyltransferase-dependent chromatin transcription. J Biol Chem **279:** 51163–51171

Bäurle I, Dean C (2008) Differential interactions of the autonomous pathway RRM proteins and chromatin regulators in the silencing of Arabidopsis targets. PLoS ONE **3:** e2733

Benhamed M, Bertrand C, Servet C, Zhou DX (2006) *Arabidopsis* GCN5, HD1, and TAF1/HAF2 interact to regulate histone acetylation required for light-responsive gene expression. Plant Cell **18:** 2893–2903

Bertrand C, Bergounioux C, Domenichini S, Delarue M, Zhou DX (2003) Arabidopsis histone acetyltransferase AtGCN5 regulates the floral meristem activity through the WUSCHEL/AGAMOUS pathway. J Biol Chem **278:** 28246–28251

Bezzubova O, Silbergleit A, Yamaguchi-Iwai Y, Takeda S, Buerstedde JM (1997) Reduced X-ray resistance and homologous recombination frequencies in a RAD54−/− mutant of the chicken DT40 cell line. Cell **89:** 185–193

Bieza K, Lois R (2001) An *Arabidopsis* mutant tolerant to lethal ultraviolet-B levels shows constitutively elevated accumulation of flavonoids and other phenolics. Plant Physiol **126:** 1105–1115

Bray CM, West CE (2005) DNA repair mechanisms in plants: crucial sensors and effectors for the maintenance of genome integrity. New Phytol **168:** 511–528

Brehm A, Miska EA, McCance DJ, Reid JL, Bannister AJ, Kouzarides T (1998) Retinoblastoma protein recruits histone deacetylase to repress transcription. Nature **391:** 597–601

Britt AB (1996) DNA damage and repair in plants. Annu Rev Plant Physiol Plant Mol Biol **47:** 75–100

Britt AB, May GD (2003) Re-engineering plant gene targeting. Trends Plant Sci **8:** 90–95

Bucceri A, Kapitza K, Thoma F (2006) Rapid accessibility of nucleosomal DNA in yeast on a second time scale. EMBO J **25:** 3123–3132

Bundock P, Hooykaas P (2002) Severe developmental defects, hypersensitivity to DNA-damaging agents, and lengthened telomeres in *Arabidopsis* MRE11 mutants. Plant Cell **14:** 2451–2462

Burnette WN (1981) "Western blotting": electrophoretic transfer of proteins from sodium dodecyl sulfate-polyacrylamide gels to unmodified nitrocellulose and radiographic detection with antibody and radioiodinated protein A. Anal Biochem **112:** 195–203

Casati P, Campi M, Chu F, Suzuki N, Maltby D, Guan S, Burlingame AL, Walbot V (2008) Histone acetylation and chromatin remodeling are required for UV-B-dependent transcriptional activation of regulated genes in maize. Plant Cell **20:** 827–842

Casati P, Stapleton AE, Blum JE, Walbot V (2006) Genome-wide analysis of high-altitude maize and gene knockdown stocks implicates chromatin remodeling proteins in response to UV-B. Plant J **46:** 613–627

Casati P, Walbot V (2004) Crosslinking of ribosomal proteins to RNA in maize ribosomes by UV-B and its effects on translation. Plant Physiol **136:** 3319–3332

Casati P, Walbot V (2008) Maize lines expressing RNAi to chromatin remodeling factors are similarly hypersensitive to UV-B radiation but exhibit distinct transcriptome responses. Epigenetics **3:** 216–229

Citterio E, Van Den Boom V, Schnitzler G, Kanaar R, Bonte E, Kingston RE, Hoeijmakers JHJ, Vermeulen W (2000) ATP-dependent chromatin remodeling by the Cockayne syndrome B DNA repair-transcription-coupling factor. Mol Cell Biol **20:** 7643–7653

Crane YM, Gelvin SB (2007) RNAi-mediated gene silencing reveals involvement of Arabidopsis chromatin-related genes in Agrobacterium-mediated root transformation. Proc Natl Acad Sci USA **104:** 15156–15161

Dubest S, Gallego ME, White CI (2004) Roles of the AtErcc1 protein in recombination. Plant J **39:** 334–342

Earley KW, Shook MS, Brower-Toland B, Hicks L, Pikaard CS (2007) In vitro specificities of Arabidopsis co-activator histone acetyltransferases: implications for histone hyperacetylation in gene activation. Plant J **52:** 615–626

Eberharter A, Becker PB (2002) Histone acetylation: a switch between repressive and permissive chromatin. EMBO Rep **3:** 224–229

Eisen JA, Sweder KS, Hanawalt PC (1995) Evolution of the SNF2 family of proteins: subfamilies with distinct sequences and functions. Nucleic Acids Res **23:** 2715–2723

Essers J, Hendriks RW, Swagemakers SM, Troelstra C, de Wit J, Bootsma D, Hoeijmakers JHJ, Kanaar R (1997) Disruption of mouse RAD54 reduces ionizing radiation resistance and homologous recombination. Cell **89:** 195–204

Friedberg EC, Walker GC, Siede W (1995) DNA Damage. ASM Press, Washington

Fritsch O, Benvenuto G, Bowler C, Molinier J, Hohn B (2004) The INO80 protein controls homologous recombination in *Arabidopsis thaliana*. Mol Cell **16:** 479–485

Gallego ME, Jeanneau M, Granier F, Bouchez D, Bechtold N, White CI (2001) Disruption of the Arabidopsis RAD50 gene leads to plant sterility and MMS sensitivity. Plant J **25:** 31–41

Gallego ME, White CI (2001) RAD50 function is essential for telomere maintenance in Arabidopsis. Proc Natl Acad Sci USA **98:** 1711–1716

Gerhardt KE, Wilson MI, Greenberg BM (1999) Tryptophan photolysis leads to a UVB-induced 66 kDa photoproduct of ribulose-1,5-bisphosphate carboxylase/oxygenase (Rubisco) in vitro and in vivo. Photochem Photobiol **70:** 49–56

Gorbunova VV, Levy AA (1999) How plants make ends meet: DNA double-strand break repair. Trends Plant Sci **4:** 263–269

Han SK, Song JD, Noh YS, Noh B (2007) Role of plant CBP/p300-like genes in the regulation of flowering time. Plant J **49:** 103–114

Hanin M, Mengiste T, Bogucki A, Paszkowski J (2000) Elevated levels of intrachromosomal homologous recombination in Arabidopsis overexpressing the MIM gene. Plant J **24:** 183–189

Hays JB (2002) *Arabidopsis thaliana*, a versatile model system for study of eukaryotic genome-maintenance functions. DNA Repair (Amst) **1:** 579–600

Hefner E, Preuss SB, Britt AB (2003) Arabidopsis mutants sensitive to gamma radiation include the homologue of the human repair gene ERCC1. J Exp Bot **54:** 669–680

Hennig L, Bouveret R, Gruissem W (2005) MSI1-like proteins: an escort service for chromatin assembly and remodeling complexes. Trends Cell Biol **15:** 295–302

Kim HJ, Hyun Y, Park JY, Park MJ, Park MK, Kim MD, Kim HJ, Lee MH, Moon J, Lee I, et al (2004) A genetic link between cold responses and flowering time through *FVE* in *Arabidopsis thaliana*. Nat Genet **36:** 167–171

Kimura S, Sakaguchi K (2006) DNA repair in plants. Chem Rev **106:** 753–766

Klein HL (1997) RDH54, a RAD54 homologue in Saccharomyces cerevisiae, is required for mitotic diploid-specific recombination and repair and for meiosis. Genetics **147:** 1533–1543

Kooistra R, Vreeken K, Zonneveld JB, de Jong A, Eeken JC, Osgood CJ, Buerstedde J-M, Lohman PHM, Pastink A (1997) The Drosophila melanogaster RAD54 homolog, DmRAD54, is involved in the repair of radiation damage and recombination. Mol Cell Biol **17:** 6097–6104

Landry LG, Chapple CCS, Last RL (1995) Arabidopsis mutants lacking phenolic sunscreens exhibit enhanced ultraviolet-B injury and oxidative damage. Plant Physiol **109:** 1159–1166

Lario LD, Ramirez-Parra E, Gutierrez C, Casati P, Spampinato CP (2011) Regulation of plant *MSH2* and *MSH6* genes in the UV-B-induced DNA damage response. J Exp Bot **62:** 2925–2937

Latrasse D, Benhamed M, Henry Y, Domenichini S, Kim W, Zhou DX, Delarue M (2008) The MYST histone acetyltransferases are essential for gametophyte development in Arabidopsis. BMC Plant Biol **8:** 121–137

Li JY, Ou-Lee TM, Raba R, Amundson RG, Last RL (1993) *Arabidopsis* flavonoid mutants are hypersensitive to UV-B irradiation. Plant Cell **5:** 171–179

Long JA, Ohno C, Smith ZR, Meyerowitz EM (2006) TOPLESS regulates apical embryonic fate in Arabidopsis. Science **312:** 1520–1523

Madronich S, McKenzie R, Caldwell M, Bjorn LO (1995) Changes in ultraviolet-radiation reaching the earth's surface. Ambio **24:** 143–152

Mazza CA, Boccalandro HE, Giordano CV, Battista D, Scopel AL, Ballaré CL (2000) Functional significance and induction by solar radiation of ultraviolet-absorbing sunscreens in field-grown soybean crops. Plant Physiol **122:** 117–126

Muris DF, Vreeken K, Schmidt H, Ostermann K, Clever B, Lohman PHM, Pastink A (1997) Homologous recombination in the fission yeast Schizosaccharomyces pombe: different requirements for the rhp51+, rhp54+ and rad22+ genes. Curr Genet **31:** 248–254

Nicolas E, Morales V, Magnaghi-Jaulin L, Harel-Bellan A, Richard-Foy H, Trouche D (2000) RbAp48 belongs to the histone deacetylase complex that associates with the retinoblastoma protein. J Biol Chem **275:** 9797–9804

Ormrod DP, Landry LG, Conklin PL (1995) Short-term UV-B radiation and ozone exposure effects on aromatic secondary metabolite accumulation and shoot growth of flavonoid-deficient Arabidopsis mutants. Physiol Plant **93:** 602–610

Pazhouhandeh M, Molinier J, Berr A, Genschik P (2011) MSI4/FVE interacts with CUL4-DDB1 and a PRC2-like complex to control epigenetic regulation of flowering time in Arabidopsis. Proc Natl Acad Sci USA **108:** 3430–3435

Pfluger J, Wagner D (2007) Histone modifications and dynamic regulation of genome accessibility in plants. Curr Opin Plant Biol **10:** 645–652

Rozen S, Skaletsky HJ (2000) Primer3 on the WWW for general users and for biologist programmers. *In* SA Krawetz, S Misener, eds, Bioinformatics Methods and Protocols: Methods in Molecular Biology. Humana Press, Totowa, NJ, pp 365–386

Sambrook J, Russel DW (2001). Molecular Cloning: A Laboratory Manual. Cold Spring Harbor Laboratory Press, Cold Spring Harbor, NY

Shaked H, Avivi-Ragolsky N, Levy AA (2006) Involvement of the Arabidopsis SWI2/SNF2 chromatin remodeling gene family in DNA damage response and recombination. Genetics **173:** 985–994

Shinohara M, Shita-Yamaguchi E, Buerstedde JM, Shinagawa H, Ogawa H, Shinohara A (1997) Characterization of the roles of the *Saccharomyces cerevisiae RAD54* gene and a homologue of *RAD54, RDH54/TID1*, in mitosis and meiosis. Genetics **147:** 1545–1556

Squatrito M, Gorrini C, Amati B (2006) Tip60 in DNA damage response and growth control: many tricks in one HAT. Trends Cell Biol **16:** 433–442

Stapleton AE, Mori T, Walbot V (1993) A simple and sensitive antibody-based method to measure UV-induced DNA damage in *Zea mays*. Plant Mol Biol Rep **11:** 230–236

Stockinger EJ, Mao Y, Regier MK, Triezenberg SJ, Thomashow MF (2001) Transcriptional adaptor and histone acetyltransferase proteins in Arabidopsis and their interactions with CBF1, a transcriptional activator involved in cold-regulated gene expression. Nucleic Acids Res **29:** 1524–1533

Sun Y, Jiang X, Price BD (2010) Tip60: connecting chromatin to DNA damage signaling. Cell Cycle **9:** 930–936

Takeda S, Tadele Z, Hofmann I, Probst AV, Angelis KJ, Kaya H, Araki T, Mengiste T, Mittelsten Scheid O, Shibahara K-I, et al (2004) BRU1, a novel link between responses to DNA damage and epigenetic gene silencing in Arabidopsis. Genes Dev **18:** 782–793

Tong H, Leasure CD, Hou X, Yuen G, Briggs W, He ZH (2008) Role of root UV-B sensing in *Arabidopsis* early seedling development. Proc Natl Acad Sci USA **105:** 21039–21044

Troelstra C, van Gool A, de Wit J, Vermeulen W, Bootsma D, Hoeijmakers JHJ (1992) ERCC6, a member of a subfamily of putative helicases, is involved in Cockayne's syndrome and preferential repair of active genes. Cell **71:** 939–953

Ulm R, Baumann A, Oravecz A, Máté Z, Adám E, Oakeley EJ, Schäfer E, Nagy F (2004) Genome-wide analysis of gene expression reveals function of the bZIP transcription factor HY5 in the UV-B response of Arabidopsis. Proc Natl Acad Sci USA **101:** 1397–1402

Vaillant I, Paszkowski J (2007) Role of histone and DNA methylation in gene regulation. Curr Opin Plant Biol **10:** 528–533

Vlachonasios KE, Thomashow MF, Triezenberg SJ (2003) Disruption mutations of ADA2b and GCN5 transcriptional adaptor genes dramatically affect *Arabidopsis* growth, development, and gene expression. Plant Cell **15:** 626–638

Wintermans JFGH, de Mots A (1965) Spectrophotometric characteristics of chlorophylls a and b and their pheophytins in ethanol. Biochim Biophys Acta **109:** 448–453

Xu L, Zhao Z, Dong A, Soubigou-Taconnat L, Renou J-P, Steinmetz A, Shen W-H (2008) Di- and tri- but not monomethylation on histone H3 lysine 36 marks active transcription of genes involved in flowering time regulation and other processes in *Arabidopsis thaliana*. Mol Cell Biol **28:** 1348–1360

Yu Y, Teng Y, Liu H, Reed SH, Waters R (2005) UV irradiation stimulates histone acetylation and chromatin remodeling at a repressed yeast locus. Proc Natl Acad Sci USA **102:** 8650–8655